

GENERATION OF A DIFFERENTIAL SIGNAL IN ZEEMAN ATOMIC ABSORPTION ANALYZER

A.B. Antipov and E.Yu. Genina

*Institute for Optical Monitoring,
Siberian Branch of the Russian Academy of Sciences, Tomsk
Received January 21, 1998*

Atomic absorption analyzers with Zeeman correction for background are widely used in analytics, geochemistry, and ecological monitoring. They outperform analyzers of other types in selectivity and sensitivity. This paper analyzes thoroughly the process of optical signal generation that can be interesting for researchers and developers. Operation of RGA-11 atomic absorption mercury analyzer with Zeeman background correction is described in detail. Possibility to significantly widen the linear section of the analyzer concentration characteristics when using the automatic regulation of amplification is demonstrated.

The operation principle of Zeeman atomic absorption analyzer is based on recording of differential absorption of Zeeman splitting spectral components of atomic radiation line by a substance under analysis. As a rule, resonance line of the analyzed substance is used as such radiation line. Zeeman components with different wavelength are transmitted in turn (usually with a polarization modulator) through the analyzed medium to a photoreceiver (PMT). The receiver, in the case of differential absorption of components, generates the varying signal corresponding to modulation and concentration of the analyzed substance.

Let us consider consistently the process of differential signal generation using the RGA-11 mercury analyzer as an example. We will consider the analyzer constructed as shown in Fig. 1 (Refs. 1 and 2).

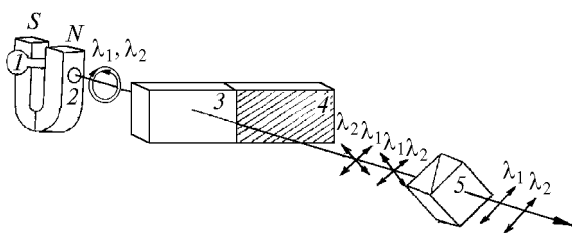


FIG. 1. The splitting scheme of Zeeman components of mercury monoisotopic radiation line at 254 nm: lamp VSB-1 (1); permanent magnet (2); photoelastic polarization modulator (3, 4); linear polarizer (Glan prism) (5); λ_1 and λ_2 are radiation wavelengths of σ^+ - and σ^- -components.

1. Radiation source is the mercury monoisotopic high-frequency electrodeless spectral line exposed to constant magnet field. The lamp emits two circular-polarized spectral components σ^+ and σ^- with different direction of electric vector rotation along lines of force of

the electric field. Optical axis of the whole analyzer is also directed along lines of force.

2. Linear polarizer set up in the beam path transmits projections of the electric vector of the components σ^+ and σ^- onto its main plane. Temporal dependence of these projections is determined by Eqs. (1) and (2)

$$E_{\sigma^+}(t) = 2^{-1/2} [\sin\omega t + \sin(\omega t + \pi/2)]; \quad (1)$$

$$E_{\sigma^-}(t) = 2^{-1/2} [\sin\omega t + \sin(\omega t - \pi/2)], \quad (2)$$

where t is time; ω is the frequency of optical oscillations.

Amplitude of linearly polarized radiation of one component is accepted as the unit amplitude of projection. Such polarization can be obtained by setting $1/4$ plate in the beam path. One axis of the plate should make an angle of 45° with the direction of oscillations transmitted by the polarizer. Hereinafter we suppose that σ -components have the same intensity and neglect the radiation losses at optical parts.

3. Let us place the polarization modulator between the source and the polarizer. The modulator is the phase plate, after passing through which the phase difference φ between two orthogonal polarization directions changes with time. In our device, we use the resonance photoelastic modulator of polarization, which operation is well described in Refs. 3–5. The modulator creates variable phase difference φ between oscillations. Direction of one oscillation coincides with the direction of modulator compression and expansion. Direction of another oscillation is normal to this direction and direction of radiation propagation. Modulation frequency f is the resonance frequency of modulator mechanical oscillations, and usually it is within 30–200 kHz, i.e. it is much smaller than the frequency of optical oscillations; ψ is modulation amplitude, rad. Temporal dependence of φ is described by the expression

$$\varphi = \psi \sin ft. \tag{3}$$

Having introduced the additional phase difference φ in Eq. (1), let us write

$$E_{\sigma^+}(t) = 2^{-1/2} [\sin(\omega t + \psi \sin ft) + \sin(\omega t + \pi/2)]. \tag{4}$$

Equation (4) can be presented as a sum of two sinusoidal oscillations with frequency ω and phase shifts φ and $\pi/2$. Such sum is sinusoid with the same frequency ω and amplitude E , which is time-dependent in our case

$$E_{\sigma^+}(t) = \{1 + \cos[\psi \sin(ft) - \pi/2]\}^{1/2}. \tag{5}$$

Similarly we can obtain the expression for σ^- -component

$$E_{\sigma^-}(t) = \{1 + \cos[\psi \sin(ft) + \pi/2]\}^{1/2}. \tag{6}$$

Equations (5) and (6) allows us to obtain the form of temporal dependence of radiation intensity I for every σ -component as square amplitude. Similar dependence can be also written for PMT current being the square receiver

$$I_{\sigma^+}(t) = \{1 + \cos[\psi \sin(ft) - \pi/2]\} I_0/2; \tag{7}$$

$$I_{\sigma^-}(t) = \{1 + \cos[\psi \sin(ft) + \pi/2]\} I_0/2, \tag{8}$$

where I_0 is intensity of one σ -component before its modulation.

Since current and intensity values are proportional to each other, then, assuming the same and constant intensity of σ -components before modulation, let us hereinafter call the optical path transmittance $T = I/I_0$ as the PMT signal. The transmittance value is modulated by photoelastic modulator and increases when an absorbing medium is in the beam path.

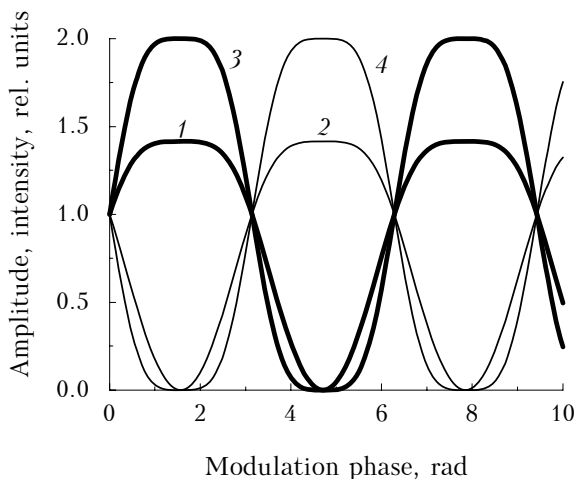


FIG. 2. Dependence of amplitude and intensity of σ^+ - and σ^- -components of Zeeman splitting passing through the photoelastic polarization modulator with modulation amplitude $\pi/2$: amplitudes of σ^+ - and σ^- -components (1 and 2), square amplitudes (3 and 4).

Temporal dependence (more precisely, dependence on the phase modulation value ft) of E and T for σ^+ -

and σ^- -components at the value of phase modulation amplitude ψ equal to $\pi/2$, corresponding to maximum signal at the resonance frequency of photoelastic modulator of polarization, is shown in Fig. 2.

Figure 3 shows the similar dependence of intensity of one σ -component at ψ varying in the range from 0 to 2π by way of $\pi/8$. It is seen from Fig. 3 that with increasing amplitude of phase difference modulation ψ the maximum variable signal is generated at the frequency f and its harmonics. Signal shape differs significantly from the sinusoidal shape of resonance oscillations of the photoelastic polarization modulator.

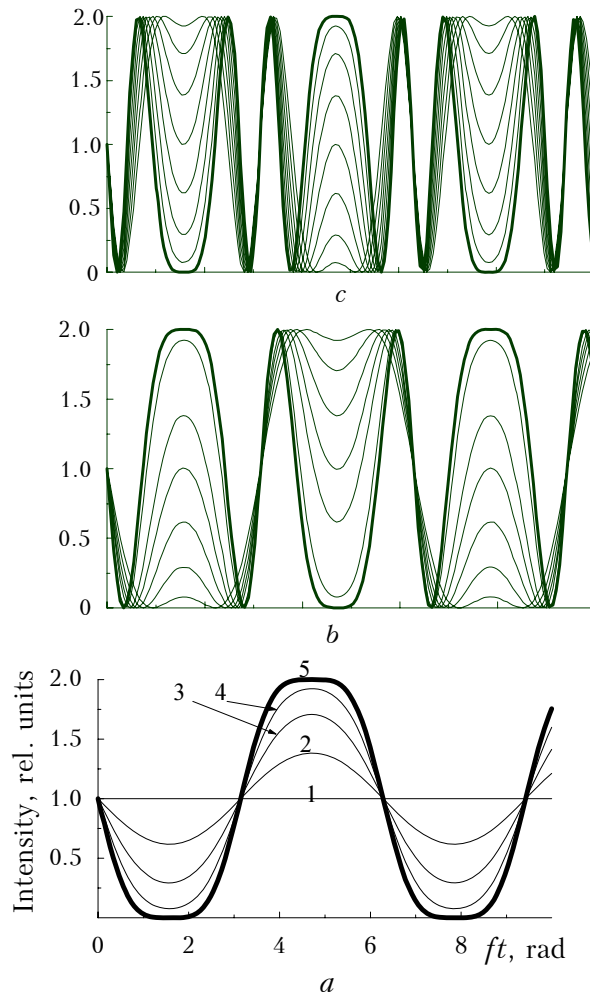


FIG. 3. Dependence of shape of variable intensity component on the amplitude ψ of modulation of phase difference between usual and unusual beams in photoelastic polarization modulator (a); $\psi = 0$ (1); $\psi = \pi/8$ (2); $\psi = \pi/4$ (3); $\psi = 3\pi/8$ (4); $\psi = \pi/2$ (5); (b and c) continuation of (a); every subsequent curve corresponds to ψ increased by $\pi/8$.

It can be readily shown that the differential signal will have just the same shape, and its amplitude will be proportional to the concentration of differentially absorbing medium in the case of weak absorption. Signals recorded in our experiment follow the shape of calculated signals. It was comparatively easy to obtain

the signal at 5th harmonic when imposing voltage of about 15 V across the photoelastic modulator at its resonance frequency (Fig. 4).

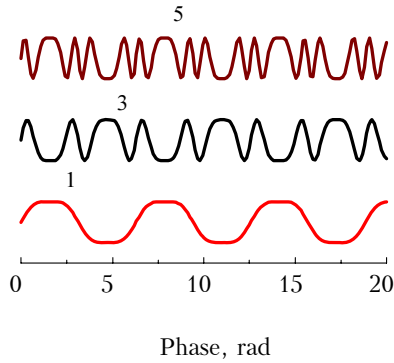


FIG. 4. Oscillogram of signal shape at 1st, 3rd, and 5th harmonics.

It is seen from Eqs. (5) and (6), as well as Figs. 2 and 3 that in the case of no absorption or the same absorption of σ^+ - and σ^- -components by the medium between the receiver and the source, the variable component of combined signal is zero

$$T = T_{\sigma^+}(t) + T_{\sigma^-}(t) = \text{const.} \tag{9}$$

In the following, this case will be referred as nonselective attenuation. Scattering, absorption by molecules, changes in transmittance of optical parts, etc. fall into this category.

Let us pass now to the differential absorption, i.e. to the most interesting case, when σ^+ - and σ^- -components are differently absorbed by medium. In our example, it is differential absorption of Zeeman components by mercury vapor. Considering that absorption follows the Bouguer law, let us write

$$T = T_{\sigma^+}(t) \exp(-\tau_{\sigma^+}) + T_{\sigma^-}(t) \exp(-\tau_{\sigma^-}), \tag{10}$$

where τ_{σ^+} and τ_{σ^-} are corresponding optical depths. Optical depth τ is the product of absorption cross section Q by concentration n of absorbing particles and beam path length in absorbing medium l .

Since σ^+ - and σ^- -components are differently absorbed by medium, for the sake of definiteness, let us rewrite Eq. (10) as Eq. (11), in which the subscript 1 corresponds to σ^- -component absorbed more strongly:

$$T = T_1 \exp(-\tau_1) + T_2 \exp(-\tau_2); \tag{11}$$

$$\tau = Qnl, \quad \tau_1 = Q_1nl, \quad \tau_2 = Q_2nl.$$

Introducing the ratio N of the smaller absorption cross section to the greater one:

$$\tau_1 = \tau \quad \text{and} \quad \tau_2 = N \tau_1 = N \tau, \tag{12}$$

we obtain

$$T = T_1 \exp(-\tau) + T_2 \exp(-N \tau). \tag{13}$$

Let us write the expression for amplitude A of the variable component of the PMT total signal. This amplitude is equal to the half difference between

maximal and minimal values of T . For $\psi = \pi/2$ (maximal PMT signal at the resonance frequency of photoelastic polarization modulator), T is maximum at $ft = \pi/2$ and minimum at $ft = 3\pi/2$. Having substituted these values into Eq. (11) with regard for Eqs. (7) and (8), we obtain the expression for the amplitude

$$A = (e^{-N\tau} - e^{-\tau})/2. \tag{14}$$

In the case of weak absorption ($N\tau; \tau \ll 1$), the amplitude A is proportional to the optical depth of one component, i.e., in fact, concentration n of differentially absorbing medium

$$A = (1 - N) Qnl. \tag{15}$$

As the concentration increases, this characteristic takes more complex form (Fig. 5, curves 6 - 10).

In our device, to eliminate the influence of nonselective absorption, the unit for automatic amplification regulation (AAR) stabilizing the constant component of PMT signal is used. In addition, AAR possesses one more valuable property. We suggest to use this property to widen the linear section of concentration characteristic of spectrophotometers operating by the method of differential absorption. Let us show how it works. Toward this aim, we divide the amplitude A by the average value of signal I_{av} (this function in our analyzer is performed by AAR)

$$I_{av} = I (e^{-N\tau} + e^{-\tau})/2; \tag{16}$$

$$A' = A/I_{av} = (e^{-N\tau} - e^{-\tau})/(e^{-N\tau} + e^{-\tau}) \tag{17}$$

or, passing to concentration,

$$A' = (e^{-Nnl\sigma} - e^{-nl\sigma})/(e^{-Nnl\sigma} + e^{-nl\sigma}). \tag{18}$$

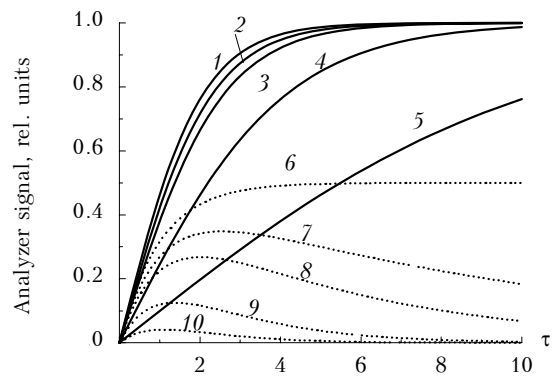


FIG. 5. Signal with AAR (solid lines) and without AAR (dashed lines) for different ratio N of absorption cross sections of Zeeman components: $N = 0$ (1, 6); 0.2 (2, 7); 0.5 (3, 8); 0.5 (4, 9); 0.8 (5, 10); τ is the optical depth for stronger absorbing component.

Dependence of A' on concentration (more precisely, on optical depth for stronger absorbing component) is shown in Fig. 5, curves 1 - 5.

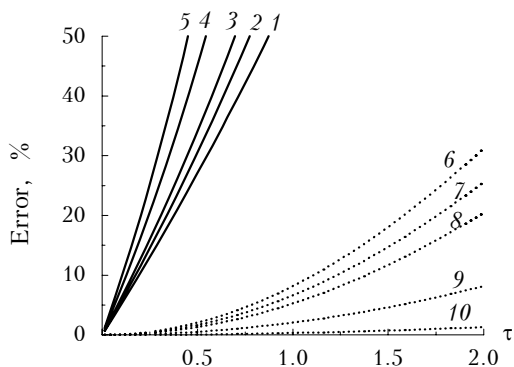


FIG. 6. Error arising when using the linear approximation. Ratio N of absorption cross sections of spectral components is denoted as in Fig. 5.

Figure 6 demonstrates the degree of widening of linear section. This figure demonstrates the errors arising for different ratio N of absorption cross section with and without AAR. For isotope ^{204}Hg used in our analyzer, the linear section (deviation from linear dependence up to 5%) widens 12 times at maximum differential absorption.

DIFFERENTIAL SIGNAL FOR ATMOSPHERIC MERCURY VAPOR

Mercury line 254 nm has the complex isotopic structure (Fig. 7), which should be taken into account when estimating the value of differential signal. We constructed spectral distribution of absorption cross section of this line using the data on isotopic composition of natural mercury and distances between components of isotopic structure,⁶⁻⁸ as well as the data on broadening and shift of the line under study by pressure.^{8,9} Dependence of spectral transmittance of atmospheric air under normal conditions on the concentration of mercury with natural isotopic composition contained in it is shown in Fig. 8. In the case when a source emits two monochromatic components, the differential signal is described by Eq. (15). In a real case, when Zeeman components are not monochromatic, transmittance of every component having passed through an absorbing medium can be presented as integral, which is the convolution of the function of spectral distribution of component $I(\nu)$ with spectral distribution of transmittance of combined profile of the natural mixture of isotopes

$$T_{\sigma^+} = \int I_{\sigma^+}(\nu) \exp[-Q(\nu - \nu_0)nl] d\nu. \quad (19)$$

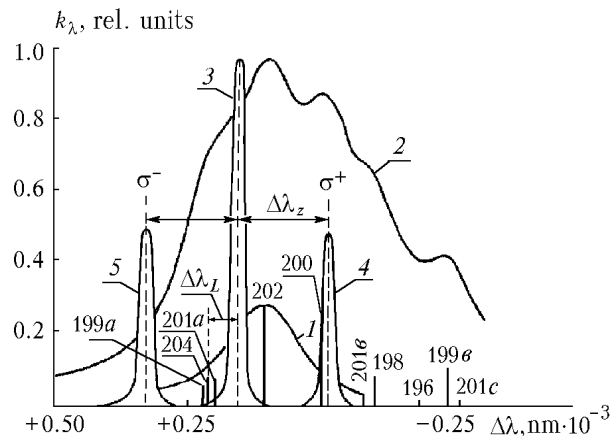


FIG. 7. Spectral characteristics of mercury atoms in the region of 254 nm: absorption line profile of ^{202}Hg isotope broadened by collisions under atmospheric pressure (1); combined profile of absorption line of atmospheric mercury isotopes (2), numbers 196–204 is for isotope nuclei masses, height of vertical bars under digits corresponds to relative intensity of isotope spectral lines; Doppler line profile emitted by mercury lamp filled with ^{204}Hg isotope (3); Zeeman splitting components of the line 3 when the lamp is exposed to longitudinal magnetic field (corresponds to maximum differential absorption (4 and 5); $\Delta\lambda_L$ is collisional shift of absorption line under atmospheric pressure.

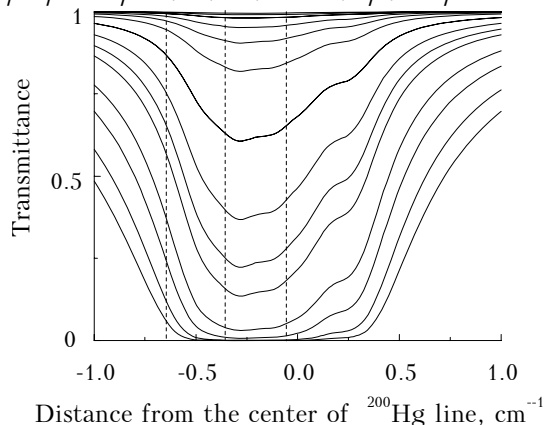


FIG. 8. Spectral transmittance of atmospheric air containing mercury vapor in the range of isotopic structure of the line at 254 nm vs. mercury vapor concentration. Transmittance curves (from top to bottom) corresponds to the following optical depth at the maximum absorption of the natural mixture of mercury isotopes: 0.005; 0.01; 0.02; 0.05; 0.1; 0.2; 0.1; 0.2; 0.5; 1; 1.5; 2; 3.5; 5; 7.5; 10. Dashed lines are for positions of σ -components at magnetic induction $b = 0.42$ T and nonsplitted line ^{204}Hg emitted by high-frequency monoisotopic lamp.

In our case, as a result of interferometric measurements, it was shown that spectral distribution of monoisotopic lamp radiation can be presented as a Doppler profile with halfwidth at half maximum $\gamma_D = 0.063 \text{ cm}^{-1}$ (hwhm). Comparison of differential signal values for monochromatic components and for components, having spectral distribution as in our case, shows that, when analyzing mercury with our analyzer, approximation of monochromatic source is quite suitable (Fig. 9).

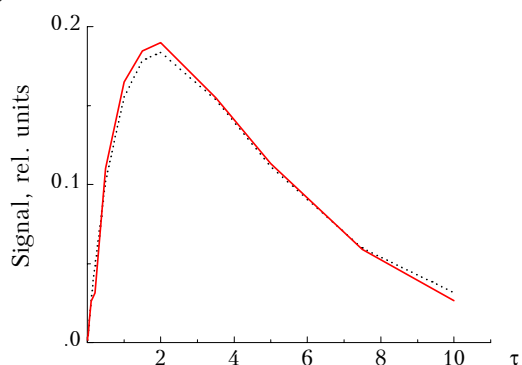


FIG. 9. Differential signal value vs. optical depth of the isotopic structure center of natural mixture of mercury isotopes. Broadening by atmospheric air under normal conditions. Solid line is for monochromatic radiation, dashed line is for the case when Zeeman components have the Doppler profile with halfwidth of 0.063 cm^{-1} , as in our experiment. Maximal deviation of differential signals does not exceed 3.5%. Combined intensity of σ -components at no absorption was taken as a unit differential signal.

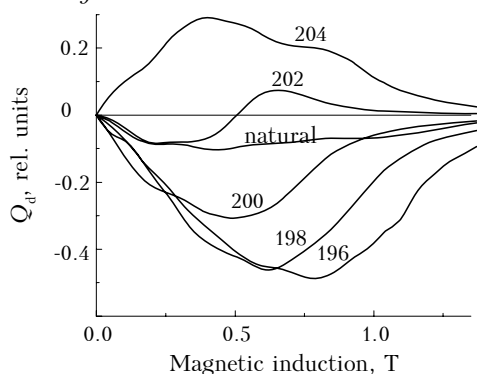


FIG. 10. Differential absorption coefficients Q_d vs. magnetic induction for VSB lamps filled with even mercury isotopes and mercury of natural isotopic composition. Spectral absorption coefficient of monoisotopic line under normal conditions is taken as Q_d . The sign of Q_d shows what σ -component is absorbed more strongly.

Differential signal of Zeeman analyzer depends on both mercury lamp filling and the value of magnetic induction (Zeeman splitting). We have computed this dependence for monoisotopic lamps with even mercury isotopes and for lamps with mercury vapor of natural isotopic composition.

Maximum differential signal is obtained when filling the lamp with ^{196}Hg isotope. Differential cross section for such a lamp is half as absorption cross section of monoisotopic line of even isotope (Fig. 10).

It should be noted that, to estimate the value of differential signal related to the mercury concentration, absorption cross sections Q expressed in relative units are used in this paper. When performing quantitative mercury analysis in samples, one must either know absolute values of Q or use standard samples (SS).

Difference between Q values from different reference books does not provide even 100% error, while mercury content in SS for low concentration may differ several times for different sets of SS. We have developed and tested for several years the calibration technique of analyzer with thin cells with saturated mercury vapor when working with liquid, solid, and gaseous samples.² In our following paper, we will consider the absolute measurements of absorption cross section of mercury vapor at wavelength of 254 nm.

REFERENCES

1. A.B. Antipov, E.Yu. Genina., G.V. Kashkan, and N.G. Mel'nikov, *Atmos. Oceanic Opt.* **7**, Nos. 11–12, 886–889 (1994).
2. M.V. Kabanov, ed., in: *Regional Monitoring of the Atmosphere. Pt. 2. New Measurement Devices and Techniques* (Spektr, Tomsk, 1997), pp. 178–196.
3. J.C. Canit and J. Badoz, *Appl. Optics* **22**, No. 4, 592–594 (1983).
4. M. Billardon and J. Badoz, *C. R. Acad. Sci. Ser. B.* **262**, 1672 (1966).
5. S.N. Jaspersen and S.E. Schnatterly, *Rev. Sci. Instrum.* **40**, 761 (1969).
6. *J. Chem. Phys.* **21**, 1762 (1952).
7. L. Bradley, *Proc. Roy. Soc.* **262**, 1308 (1961).
8. S.E. Frish, *Optical Spectra of Atoms* (Fizmatgiz, Moscow, 1963).
9. F. Schuller and W. Behmenburg, *Physics Reports (Section of Physics Letters)* **12**, No. 4, 273–334 (1974).